ASTFE
American Society
of Thermal and Fluids Engineers

8th Thermal and Fluids Engineering Conference (TFEC)
May, 2023
Partially Online Virtual and at University of Maryland, MD

TFEC-2023-xxxxx

CALIBRATION OF A 1D EJECTOR MODEL FROM FULL-SCALE EXPERIMENTS

J. Van den Berghe,[1,*,2,*] M. Delsipee,[1] P. Planquart,[1] Y. Bartosiewicz,[2] M. A. Mendez[1]

[1]von Karman Institute for Fluid Dynamics (VKI)
Waterloosesteenweg 72, 1640 Sint-Genesius-Rode, Belgium
[2]Institute of Mechanics, Materials, and Civil Engineering (iMMC)
Université catholique de Louvain (UCLouvain), 1348 Louvain-la-Neuve, Belgium

ABSTRACT

We present the calibration of a 1D ejector model on experimental data from a large-scale ejector facility at the von Karman Institute. The facility allows for adjusting the inlet pressures (with pressure ratios up to 5) and temperatures (with temperature ratios up to 1.6) and producing mass flow rates up to 0.7 kg/s. The experimental data are used to calibrate an ejector model consisting of two interacting 1D domains based on the compound choking theory. The model closure is carried out in terms of friction factor for the primary flow and a variable loss coefficient for the secondary flow. These were successfully linked to the ratios of inlet and outlet pressures, allowing the calibrated model to predict both mass flow rates with 10 % accuracy.

KEY WORDS: ejector modeling, closure relations, large-scale experiments

1. INTRODUCTION

Ejectors are devices to entrain a flow without moving parts. The entrainment is driven by a primary flow that expands through a nozzle in a low-pressure mixing chamber, followed by a diffuser to recover pressure in both the primary and the entrained (secondary) flow. Their simple operating principle makes ejector fundamental components in aeronautics, energy production, refrigeration and the processing industry for mixing, suction and compression. Nevertheless, ejectors exhibit complex flow phenomena, such as shock trains and turbulent mixing, that make their high-fidelity simulation very costly. On the other hand, engineering 0D and 1D models seek to lump these local effects in closure coefficients, such as isentropic efficiencies or friction coefficients, to produce fast predictions of the ejector performances. However, the calibration of these coefficients requires a large amount of data and is often valid only within a narrow range of operating conditions [2].

In this work, we present the calibration of a 1D ejector model on an extensive experimental database collected from a large-scale ejector facility. Moreover, we identify a relation linking the closure coefficients to the operating conditions, thereby extending the robustness of the 1D model. The ejector model is discussed in section 2. The experimental facility is detailed in section 3, along with the data used for the calibration in section 4. The results are shown in section 5, with a conclusion in section 6.

2. EJECTOR MODEL

The model used in this work is a simplified version of the 1D ejector model by Banasiak and Hafner [1]. The ejector are treated as 1D domains. The pre-mixing chamber is treated in 0D and the pressure in the primary and secondary flow are assumed to be equal at the inlet of the constant-area section of the mixing pipe.

*Corresponding J. Van den Berghe: jan.vandenberghe@vki.ac.be

We simplify the model by removing the mass exchange and the corresponding terms in the momentum and energy equations. Together with the assumption of equal static pressure, this simplification allows a natural connection to the compound choking theory for ejectors [4]. In particular, the on-design calculation procedure enforces the compound choking indicator β to equal zero at the inlet of the mixing pipe. Downstream, the equations admit a subsonic and a supersonic solution. On the design point, the subsonic solution is retained to recover the maximal back pressure that chokes the flow, while at lower back pressures, the flow expands farther and becomes subsonic through a normal shock. As opposed to 0D models, the shock position can be resolved to match the back pressure.

Finally, we consider an ideal gas (air) and zero friction in the mixing pipe, so the only remaining source term in the mixing region remains the shear stress between the two streams, which reads: $\tau = [(\rho_p + \rho_s)/2][(v_p + v_s)(v_p - v_s)]/(4\sigma\sqrt{\pi})$, where ρ is the density, v is the speed, the subscripts p and s denote the primary and secondary section and σ is the spreading rate of the primary jet [3]. In this work, σ is fixed to 13, because its local effect on the mixing between the streams can not be assessed from global mass flow rate measurements. Its calibration from pressure taps or from CFD will be the subject of future investigation. The remaining closure coefficients are the friction coefficient f_p for the primary nozzle and a secondary total pressure loss $\Delta p_{t,s}$, which is introduced upstream of the secondary domain. In practice, the secondary losses are distributed in the ejector, but the experimental data do not allow to localize the losses. Introducing the complete loss at the secondary inlet is thus a modeling choice. The extended version of this work will report on the complete formulation of the model.

3. EXPERIMENTAL SETUP

Figure 1 shows a sketch of the experimental facility. Compressed air is supplied on the top left. The inlet pressures are then regulated independently, allowing to set inlet pressure ratios $\Pi_2 = p_{t,s}/p_{t,p}$ between 0.2 and 1, with a maximal pressure of 5 bar. A 150 kW heater can heat one of the inlets up to a temperature of 200 °C. The uncertainty on the measured pressures is 1375 Pa and 1 °C on the temperatures. The flow settles through 2.5 m long straight pipes before passing through two vortex mass flow meters, which have an accuracy of 2 % of the full range (1 kg/s in the current configuration). The maximal achievable flow rate of the facility is 0.7 kg/s. Two flexible tubes allow to connect the heated inlet either to the primary or the secondary inlet of the ejector, which is located on the far right. Both inlets and the outlet are instrumented with four thermocouples and a pressure transducer connected to four pressure taps. With the measured mass flow rates and the known cross-section, these static quantities can be converted to their total counterparts to serve as boundary conditions in the numerical model. Finally, a manual valve at the diffuser exit allows to manipulate the back pressure.

The measured primary and secondary mass flow rates are shown on figure 2 as a function of the back pressure ratio $\Pi_1 = p_d/p_{t,p}$ and the inlet pressure ratio Π_2. The uncertainties on the pressure ratios are obtained through classic propagation. All the data points consider a choked primary nozzle so the back pressure does not influence the primary flow (cf. figure 2a). The secondary mass flow rate remains constant at low back pressures, but decreases with increasing back pressure in the off-design regime (cf. figure 2b). High secondary inlet pressures increase the mass flow rate and the back pressure of the on-design point.

4. CALIBRATION STRATEGY

To discover correlations between the closure coefficients f_p and $\Delta p_{t,s}$ and the pressure ratios Π_1 and Π_2 (cf. section 2), each point was considered separately. Because the primary nozzle is choked, we first calibrate the primary friction coefficient f_p by penalizing the prediction error on the primary mass flow rate $\dot{m}_p$ on the *complete* dataset.

Next, the procedure continues point by point depending on the operating conditions. In on-design conditions, we impose $\beta = 0$ at the inlet of the mixing pipe and the parameter $\Delta p_{t,s}$ is calibrated by penalizing the

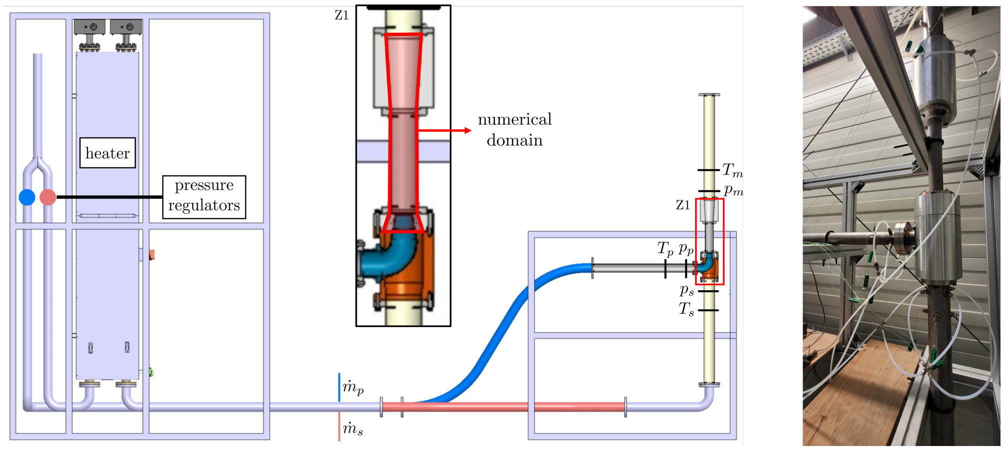

Fig. 1 Schematic overview of the experimental facility with individual inlet pressure regulators, one heated line, vortex mass flow meters and pressure and temperature sensors at the ejector inlets and outlet.

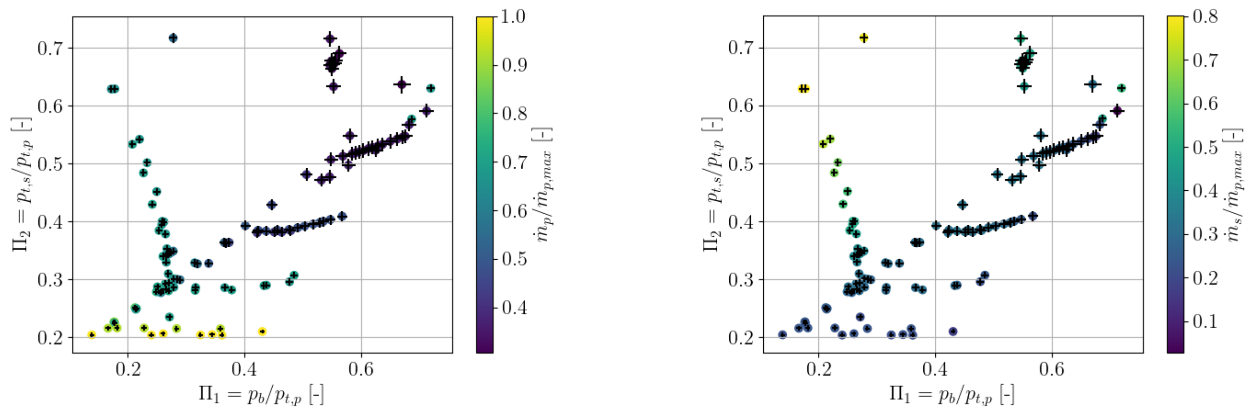

(a) Primary mass flow rate

(b) Secondary mass flow rate

Fig. 2 Experimental mass flow rates in function of the two pressure ratios. The black crosses indicate the uncertainty on the inlet conditions and the uncertainty on the mass flow rate is 0.02 kg/s.

prediction error on the secondary mass flow rate. The back pressure at the design point follows from the subsonic solution in the mixing pipe and the shock position can be determined similarly as for a classic 1D nozzle. In off-design conditions, the compound choking indicator β depends on the back pressure and becomes positive at the inlet of the mixing pipe. Both β and $\Delta p_{t,s}$ are found iteratively by penalizing the prediction error on the secondary mass flow rate $\dot{m}_s$ *and* the back pressure p_d.

5. RESULTS

The primary friction coefficient was calibrated on the complete dataset, leading to $f_p = 0.0017$. The calibrated secondary pressure losses $\Delta p_{t,s}$ are shown on figure 3a and correlate with the secondary mass flow rate (cf. figure 2b). Higher friction could explain this result, but more local data is required to determine the source of the losses with more certainty. The corresponding mass flow rates are shown on figure 3b with the experimental uncertainty in x and the numerical uncertainty in y, which is obtained by propagating the uncertainties on the operating conditions. The predictions fall within an error margin of 10 %, indicated by the dashed lines. The numerical uncertainty is higher on the secondary mass flow rate compared to the primary due to the sensitivity to the back pressure in off-design operation. Note that $\Delta p_{t,s}$ evolves continuously in the plane of pressure ratios, independently of the inlet temperature ratio.

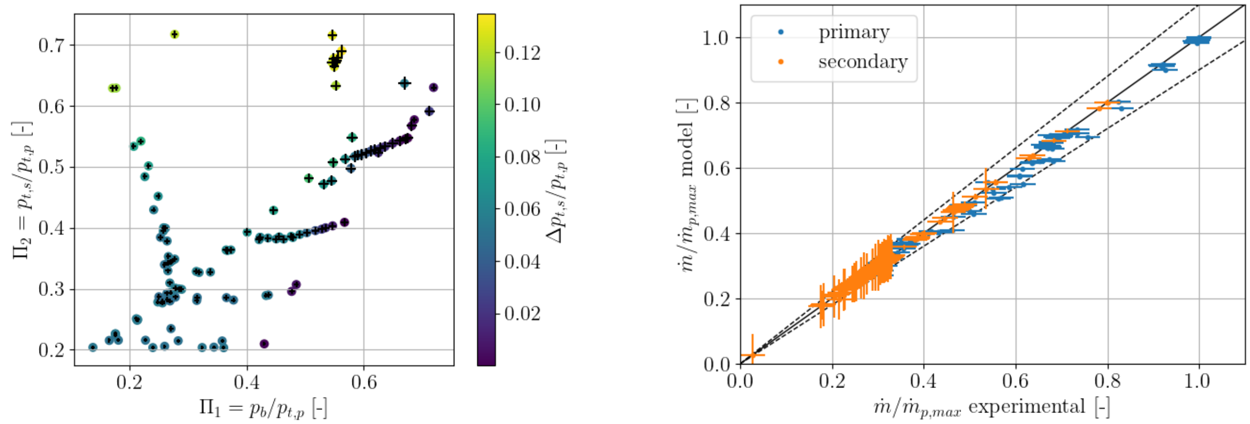

(a) Result of the calibration of $\Delta p_{t,s}$

(b) Primary and secondary mass flow rate

Fig. 3 Calibration result for the secondary pressure loss $\Delta p_{t,s}$ (left) and comparison of the mass flow rates from the calibrated model and from the experiments (right). The dashed lines indicate a 10 % error margin.

6. CONCLUSION

We proposed a calibration procedure for a modified 1D ejector model based on the compound choking theory. The model was calibrated on an experimental dataset in a wide range of conditions for a single large-scale ejector. As a result, both mass flow rates were predicted with an accuracy of 10 %, and the resulting correlation of the secondary losses with the inlet and outlet pressure ratios makes physical sense. It can therefore be envisaged to apply the method to ejectors with different geometries to include area ratios in the analysis. Furthermore, wall pressure measurements in the mixing pipe or CFD will help to extend the procedure with the spreading rate of the primary jet, hence further localizing the losses and increasing the fidelity of local predictions of the 1D model.

ACKNOWLEDGMENTS

This project has received funding from the Clean Sky 2 Joint Undertaking (JU) under grant agreement No 101008100. The JU receives support from the European Union's Horizon 2020 research and innovation programme and the Clean Sky 2 JU members other than the Union.

Horizon 2020 European Union Funding for Research & Innovation

Clean Sky 2 JOINT UNDERTAKING

Disclaimer: The contents presented in this article reflect only the author's point of view: the authors and Clean Sky JU are not responsible for any use that may be made of the information it contains.

REFERENCES

[1] Banasiak, K. and Hafner, A., "1d computational model of a two-phase r744 ejector for expansion work recovery," *International Journal of Thermal Sciences*, 50(11), pp. 2235–2247, (2011).

[2] Besagni, G., Mereu, R., Chiesa, P., and Inzoli, F., "An integrated lumped parameter-cfd approach for off-design ejector performance evaluation," *Energy Conversion and Management*, 105, pp. 697–715, (2015).

[3] Clark, L., "Application of compound flow analysis to supersonic ejector-mixer performance prediction," *33rd Aerospace Sciences Meeting and Exhibit*, p. 645, (1995).

[4] Lamberts, O., Chatelain, P., Bourgeois, N., and Bartosiewicz, Y., "The compound-choking theory as an explanation of the entrainment limitation in supersonic ejectors," *Energy*, 158, pp. 524–536, (2018).